J Prosthodont Res. 2023; 67(4): 626–632

OPEN ACCESS

Journal of Prosthodontic Research

Original article

Comparison of the fatigue life of pure titanium and titanium alloy clasps manufactured by laser powder bed fusion and its prediction before manufacturing

Kento Odaka [a], Shota Kamiyama [b], Hideo Takizawa [c], Naoki Takano [d], Satoru Matsunaga [e,*]

[a] Department of Oral and Maxillofacial Radiology, Tokyo Dental College, Tokyo, Japan, [b] Graduate School of Keio University, Yokohama, Japan, [c] Mechanical Engineering Department, Nippon Institute of Technology, Miyashiro, Japan, [d] Department of Mechanical Engineering, Keio University, Yokohama, Japan, [e] Department of Anatomy, Tokyo Dental College, Tokyo, Japan

Abstract

Purpose: In this study, the fatigue properties of additively manufactured titanium clasps were compared with those of commercially pure titanium (CPTi) and Ti–6Al–4V (Ti64), manufactured using laser powder-bed fusion.

Methods: Fourteen specimens of each material were tested under the cyclic condition at 1 Hz with applied maximum strokes ranging from 0.2 to 0.5 mm, using a small stroke fatigue testing machine. A numerical approach using finite element analysis (FEA) was also developed to predict the fatigue life of the clasps.

Results: The results showed that although no significant differences were observed between the two materials when a stroke larger than 0.35 mm was applied, CPTi had a better fatigue life under a stroke smaller than 0.33 mm. The distributions of the maximum principal stress in the FEA and the fractured position in the experiment were in good agreement.

Conclusions: Using a design of the clasp of the present study, the advantage of the CPTi clasp in its fatigue life under a stroke smaller than 0.33 mm was revealed experimentally. Furthermore, the numerical approach using FEA employing calibrated parameters for the Smith–Watson–Topper method are presented. Under the limitations of the aforementioned clasp design, the establishment of a numerical method enabled us to predict the fatigue life and ensure the quality of the design phase before manufacturing.

Keywords: Fatigue life, Additive manufacturing, Pure titanium, Titanium alloy, Finite element analysis

Received 4 August 2022, Accepted 13 February 2023, Available online 8 April 2023

1. Introduction

Additive manufacturing (AM), which is also known as three-dimensional (3D) printing, is a new manufacturing method that allows the fabrication of patient-dependent medical devices with a short turnaround time. Among the various AM techniques, laser powder bed fusion (LPBF) has been extensively studied and used[1]. AM has been widely used in the engineering field for the production of automobiles, airplanes, industrial machines, and consumer products. However, its applications in medical sector have also been increasing, accounting for 11.3% of the total number of AM applications[2,3].

The casting of Co–Cr alloys has been widely used in the medical field[4–6]. Several studies have been conducted on the use of AM for the production of Co–Cr clasps, including the evaluation of static bending[7], geometrical accuracy[8,9], surface roughness[9,10], internal porosity[10], and fatigue behavior[11–13]. Kato *et al.*[11] measured the retentive force under cyclic loading up to 10^4 cycles, which is a clinically relevant number of cycles. They found that after 10^3 cycles, the retentive force decreased from 10 N to approximately 6 N and remained approximately constant up to 10^4 cycles. Zhang *et al.*[12] and Schweiger *et al.*[13] found no significant differences in the fatigue behavior between cast and AM Co–Cr clasps. Schweiger *et al.*[13] also reported that the initial retentive force of an AM clasp was 15.74 N, which was higher than that of a cast clasp. They also reported that the survival rate of AM clasps after 65,000 cycles was higher than that of cast clasps.

Ti has a significant potential for the AM using LPBF[14]. Before the widespread application of AM, a study was conducted to compare the properties of Co–Cr and Ti–6Al–7Nb (Ti67)[15]. Takayama *et al.*[16] reported positive clinical data regarding the use of titanium dentures, particularly pure titanium. Among recent studies using the AM of commercially pure titanium (CPTi) and Ti–6Al–4V (Ti64), the study by Takahashi *et al.*[17] demonstrated that the initial retentive forces of cast CPTi and cast Ti64 were identical, and those of AM CPTi were slightly smaller than those of AM Ti64 but better than those of casted CPTi and cast Ti64. The retentive forces with up to 10^4 insertion/removal cycles of AM CPTi were higher than those of AM Ti64 and AM Ti67 considering the averaged values; however, the variability was slightly larger. Surface roughness is another critical factor in AM. Takahashi *et al.*[17] found that the surface of AM CPTi was better than those of AM Ti64 and AM Ti67. Although the yield stress and ultimate strength of CPTi are lower than those of Ti64, additively

DOI: https://doi.org/10.2186/jpr.JPR_D_22_00207
***Corresponding author:** Satoru Matsunaga, Department of Anatomy, Tokyo Dental College 2-9-18 Kandamisaki-cho, Chiyoda-ku, Tokyo 101-0061, Japan.
E-mail address: matsuna@tdc.ac.jp

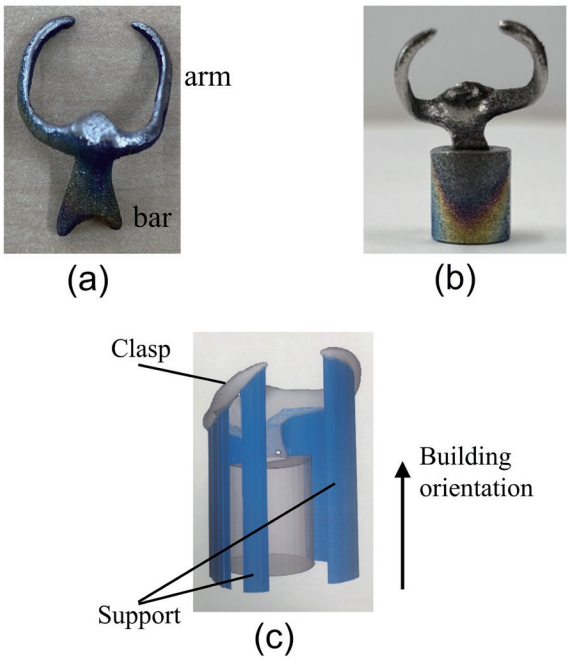

Fig. 1. Additively manufactured clasp specimen. (a): Additively manufactured clasp of commercially pure titanium (CPTi) and ti-6A1-4V (Ti64). (b): Clasp specimen for fatigue test with cylindrical chucking part. (c): Building-orientation and support structure for laser power bed fusion process.

manufactured CPTi exhibits a significant application potential.

This study investigates the fatigue properties of titanium clasps by comparing CPTi and Ti64 for up to 10^5 cycles. In addition to the experimental study, a numerical approach using finite element analysis (FEA) is presented to predict the fatigue life of CPTi and Ti64 clasps before manufacturing. The need for numerical studies using FEA is increasing owing to the demand for the quality assurance of AM products[18–20] and for the design of new medical devices[21]. In the Materials and methods section, the design of the clasp specimens is presented, followed by the fatigue test method and the numerical strategy using the elastoplastic material model, finite element model, and fatigue life prediction method.

2. Materials and Methods

2.1. Design of the clasp specimen

In this study, a typical Aker clasp for the second molar was selected as the model. The clasp shown in **Figure 1a** was additively manufactured via LPBF using an EOS M290 printer (EOS, Munich, Germany). The dimensions of the clasp specimens are listed in **Table 1**. CPTi and Ti64 were used for EOS M290. Specifically, EOS CPTi grade 2 particles with a maximum size of 38–45 μm on average were sieved before manufacturing. The layer pitch was 30 μm for both materials. In general, in the LPBF process, the particle size should be compatible with the layer pitch.

A cylindrical chucking part was designed to chuck the clasp for the fatigue test, as shown in **Figure 1b**. The building orientation and support structure are shown in **Figure 1c**. The process was monitored and recorded with the help of a printing service engineering company (J-3D Co., Ltd., Nagoya, Japan). No post-treatment methods were employed, and the as-manufactured specimens were used for the fatigue tests.

Table 1. Design of the clasp specimen

	(mm)
Thickness of the clasp shoulder	1.5
Width of the clasp shoulder	3.0
Thickness of the middle of the clasp arm	1.0
Width of the middle of the clasp arm	1.7
Thickness of the clasp tip	0.5
Width of the clasp tip	0.7
Length of the arm	14.0

2.2. Fatigue test

A small stroke fatigue testing machine IMC-0608 (Imoto Machinery, Kyoto, Japan), as shown in **Figure 2a**, was used. **Figures 2b and c** illustrate the chucking jig and the loading device for one arm of the clasp, respectively. The fatigue testing machine was stroke-controlled, and the reaction force was measured.

Fourteen specimens of each material were tested under cyclic conditions at 1 Hz with an applied maximum stroke δ as defined in **Figure 2d**. δ is a constant for each stroke-controlled fatigue test. In this study, δ ranged from 0.2 to 0.5 mm. To determine the fatigue life, the N25 test was employed that defines the fatigue life when the reaction force was reduced to 75% of the initial force.

2.3. Elasto-plastic material model for FEA

The material properties of CPTi and Ti64 were evaluated using five dumbbell-type flat-plate specimens for each material, as shown in **Figure 3**. The specimens were manufactured using an EOS M290 printer. Based on the obtained relationship between the true stress and plastic strain, the Swift hardening law in Eq. (1) was defined for elastoplastic FEA.

$$\bar{\sigma} = C\left(\alpha + \overline{\varepsilon^p}\right)^n \tag{1}$$

where $\bar{\sigma}$ is the von Mises stress; $\overline{\varepsilon^p}$ is the equivalent plastic strain; *C*, *a*, and *n* are the coefficients to be calibrated using the experimental results.

2.4. Finite element model

Elastoplastic FEA was performed by simulating the experiment using the Swift hardening law. The computer- aided design model in the STL data format for the LPBF was used for finite element modeling. The constrained condition was set at the surface of the cylinder, and the prescribed displacement was applied, as illustrated in **Figure 4a**. The displacement vector and surface nodes for applying the prescribed displacement were determined using a picture of the experimental setup. A commercial FEA code, COMSOL Multiphysics ver.5.5 (COMSOL, Inc., USA), was used. A finite-element mesh was generated using accurate 10 node tetrahedral elements, as shown

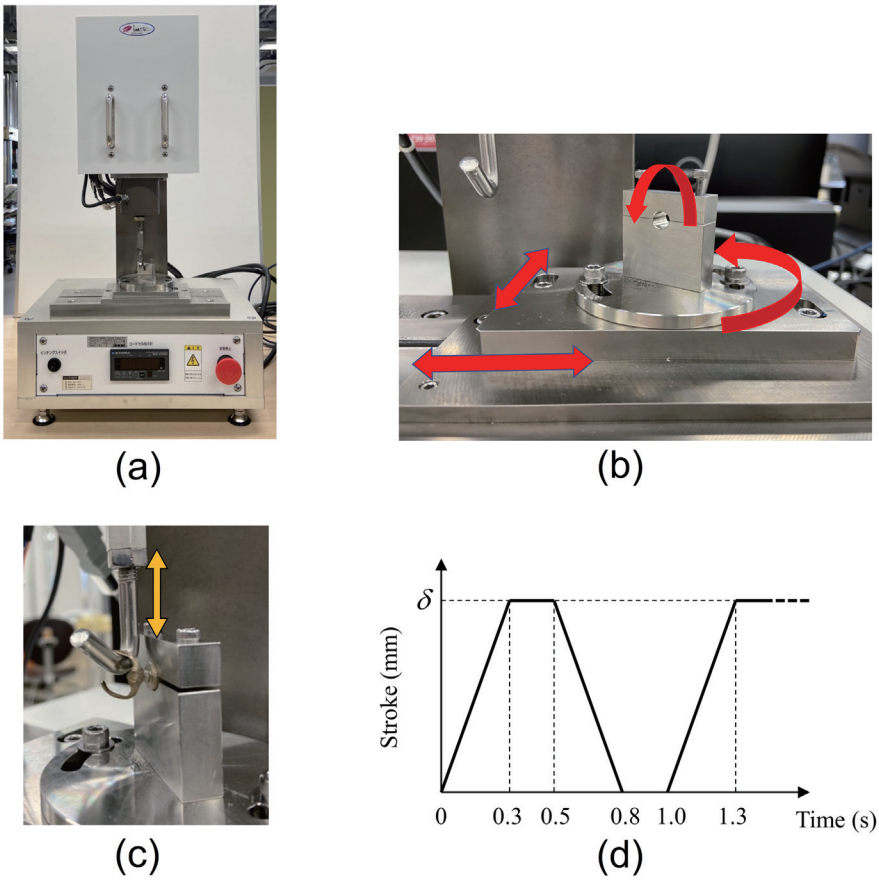

Fig. 2. Fatigue testing machine. (a): Small stroke fatigue testing machine IMC-0608 (Imoto Machinery, Kyoto, Japan). (b): Chucking jig for clasp specimen. (c): Loading device for one arm of clasp. (d): Applied cyclic stroke.

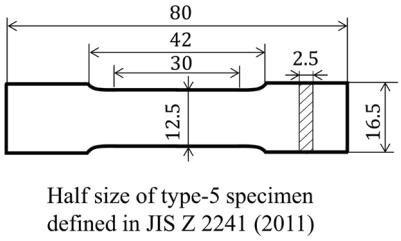

Fig. 3. Dumbbell-type specimen to measure material properties of CPTi and Ti64

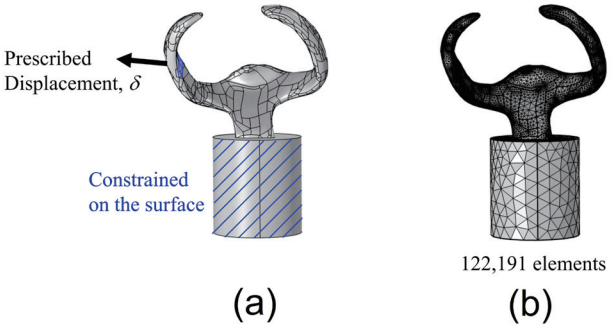

Fig. 4. Finite element model of the fatigue test specimen. (a): Solid model of clasp made from STL data with cylindrical chucking part and boundary conditions. (b): Finite element mesh using 10 node tetrahedral elements.

in **Figure 4b**.

2.5. Prediction of the fatigue life

The maximum principal stress and maximum principal strain obtained via FEA were used for the prediction of the fatigue life using the Smith–Watson–Topper (SWT) method[22] expressed by Eq. (2).

$$\frac{\Delta\varepsilon}{2}\sigma_{max} = \frac{(\sigma'_f)^2}{E}(N_f)^{2b} + \sigma'_f\varepsilon'_f(N_f)^{b+c} \quad (2)$$

where N_f is the fatigue life, and E is the Young's modulus. The calculated maximum principal stress was used for determining σ_{max}, and the maximum principal strain was used for estimating $\Delta\varepsilon$[20]. Based on the rule of Baumel and Seeger[23], $\sigma'_f = 1.67\sigma_u$ and $\varepsilon'_f = 0.35$ were used, where σ_u is the ultimate strength. Parameters b and c were calibrated in this study for CPTi and Ti64, respectively.

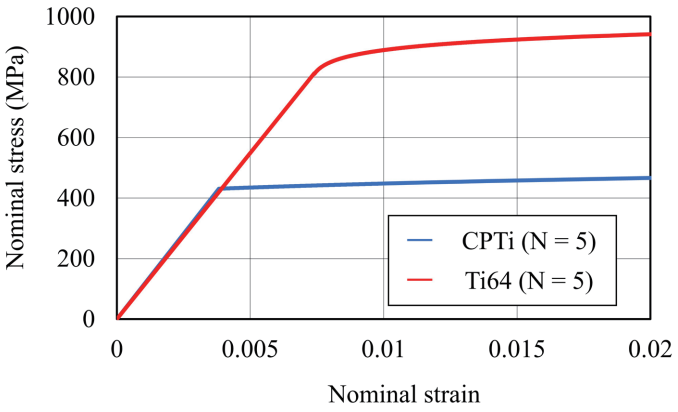

Fig. 5. Static tensile test results for CPTi and Ti64, in which the curve shows the average of 5 specimens for each material

Table 2. Measured material properties and coefficients of Swift hardening law for finite element analysis

	CPTi	Ti64
Young's modulus *E* (GPa)	112.7	109.8
Yield stress σ_Y (MPa)	431	813
Ultimate strength σ_u (MPa)	527	936
C (MPa)	647.5	1111
n	0.0915	0.038
a	0.0117	0.00025

3. Results

3.1. Material properties

From the static tensile test of dumbbell-type flat plate specimens of CPTi and Ti64, the relationship between stress and strain was obtained, as shown in **Figure 5**. The curve shows the average of the results obtained for five specimens. The variability was negligible for both materials. The Young's modulus, yield stress, ultimate strength, and coefficients of the Swift hardening law in Eq. (1) were calibrated, as summarized in **Table 2**.

The Young's moduli of CPTi and Ti64 were approximately the same. The yield stress and ultimate strength of Ti64 are approximately double those of CPTi.

3.2. Experimental and numerical results for the fatigue life

To explain the fatigue behavior, **Figure 6** shows a typical example of the distribution of the maximum principal stress in the FEA and the fractured position in the experiment. These results were obtained when the stroke was 0.5 mm, which was the maximum value in this study. Therefore, the fatigue life of the specimen was only 6878. For all specimens, the fracture position was approximately the same in all the experiments, which was consistent with the stress concentration region in the FEA.

Figure 7 shows the method for determining the fatigue life based on the N25 test method. Two results obtained for CPTi under 0.30 and 0.35 mm stroke conditions are shown. The reaction force gradually decreased by 10% of the initial force and then rapidly decreased.

The experimentally obtained fatigue life of a total of 28 specimens is plotted in **Figure 8**; the circular and triangular markings represent values obtained for CPTi and Ti64, respectively. For both materials, when the applied stroke was less than 0.33 mm, no significant variability was observed. The dashed lines represent the approximated curves. If 10^4 cycles were required for clinical use, the allowable stroke was less than 0.45 mm for both materials. When a stroke smaller than 0.33 mm was applied, CPTi had a better fatigue life than Ti64. For strokes larger than 0.35 mm, no clear differences were observed in the fatigue life between CPTi and Ti64.

Using the approximated dashed curves, the parameters of the SWT method in Eq. (2) were calibrated as listed in **Table 3**. The calibrated parameters enable the prediction of the fatigue life before manufacturing in the design phase of patient-specific clasps with different shapes.

4. Discussion

Comparing the experimentally obtained fatigue life of CPTi and Ti64 clasps, no significant differences were observed between the two materials when a stroke larger than 0.35 mm was applied. However, CPTi had a better fatigue life under a stroke smaller than

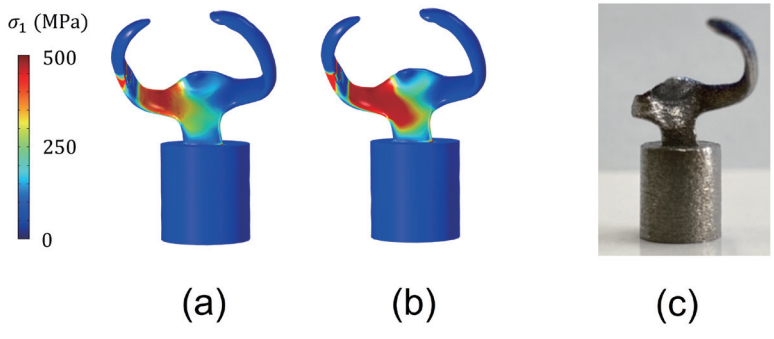

Fig. 6. Maximum principal stress distribution at a prescribed displacement d = 0.5 mm and fractured fatigue test specimen after 6878 cycle stroke of 0.5 mm. (a): CPTi. (b): Ti64. (c): Fractured CPTi specimen.

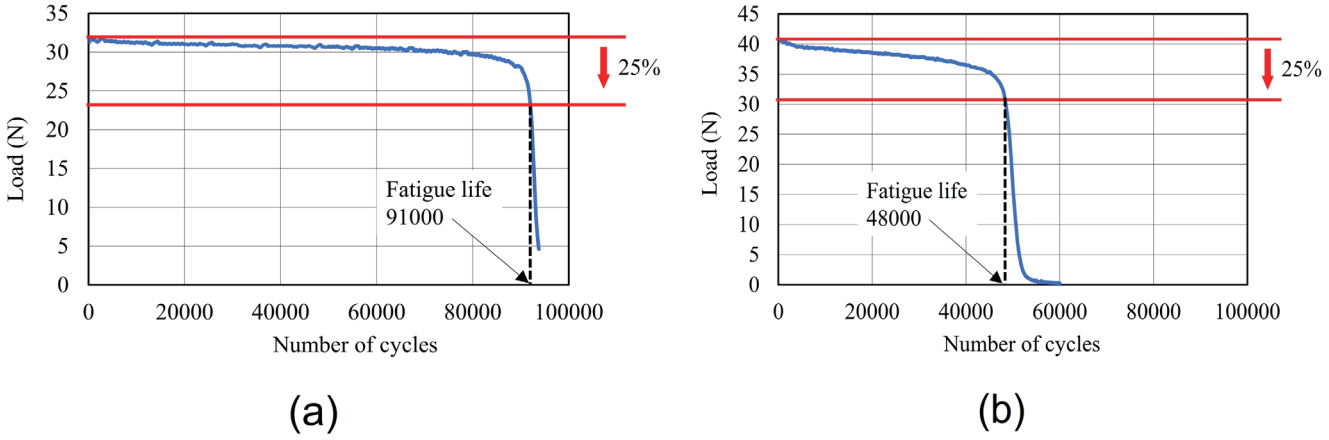

Fig. 7. Time history of the reaction force and the determination of the fatigue life using the N_{25} method. (a): CPTi specimen under 0.30 mm stroke. (b): CPTi speciment under 0.35 mm stroke.

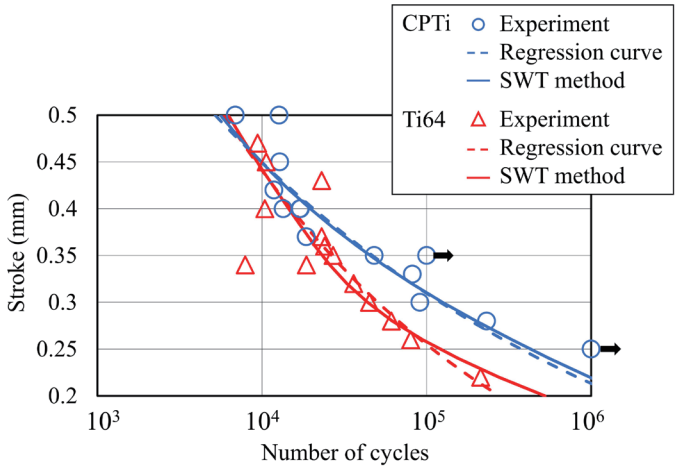

Fig. 8. Experimentally obtained fatigue life of CPTi and Ti64 clasps with each regression curve and prediction obtained using the Smith–Watson–Topper (SWT) method employing calibrated parameters

Table 3. Calibrated fatigue parameters in the equation used in the Smith–Watson–Topper method

	CPTi	Ti64
b	-0.067	-0.105
c	-0.419	-0.453

0.33 mm. In this smaller stroke range, the fatigue life of both materials exceeded 10^4 cycles and that of CPTi under a stroke of ≤0.3 mm exceeded 10^5 cycles. In a study of Co–Cr clasps by Marie *et al.*[6], the measured clasp tip displacements ranged from 0.105 to 0.319 mm. Tan *et al.*[24] observed permanent deformation in their fatigue tests after a critical crack appeared in the middle of the arm. The largest displacement (>0.5 mm) was observed at the clasp tip; however, the displacement at the middle position where the crack was observed was approximately 0.1 mm. The boundary condition in our experiment varies from that of the real case or previously published studies[6,24]. However, the stroke range at the middle position of the arm is consistent with those reported by other researchers. Therefore, a notable finding of this study is the good performance of CPTi in terms of the fatigue behavior. In future, the clinical evidence of partial dentures with CPTi clasps, as presented by Fueki *et al.*[25], should be determined.

The potential of AM has been reported in many papers[11–13] through comparison with casted clasps. However, they are mainly focused on Co–Cr clasps. For titanium clasps produced via AM, as described in the Introduction, Takahashi[17] reported that CPTi and Ti64 produced via AM showed higher retentive forces than those of casting at both initial states and after 10^4 insertion and removal cycles. The initial retentive force of the CPTi AM clasp was slightly lower than that of Ti64, which agreed with our results for a large stroke. In addition, our study reveals the advantages of using CPTi in the high-cycle region. However, no control specimens were prepared, such as cast titanium clasps or conventional Co–Cr clasps with the same shape and size, which is a limitation of this study. Process-induced defects and surface conditions should also be examined in future studies. Additionally, the effects of the difference in the crystallite structures of CPTi and Ti64 on the fatigue behavior should be explored.

Many studies have demonstrated the high potential of CPTi fabricated via LPBF[14,16,17,26]. In our study, grade 2 pure Ti (EOS, Munich, Germany) was used in the same manner as that described by De Wild *et al.*[26]. Takayama *et al.*[16] used JIS type 3 pure titanium. The yield stress value listed in **Table 1** is equivalent to the value of the better grade 4 specimen presented in[14]. Another possibility for obtaining improved pure titanium was presented in[14], to achieve a higher yield stress and similar elongation to those of Ti64. In addition to the static properties of CPTi, we demonstrated the merit of CPTi in terms of a high-cycle fatigue life. Note that the properties of Ti64 are discussed in our previous paper on FEA[20].

Considering the surface roughness, which is assumed to exhibit a correlation with fatigue behaviors, Takahashi *et al.*[17] reported that CPTi possessed a better surface morphology than Ti64 and Ti67. As described in Section 2.2, specimens manufactured without the post-treatment step were used in our study. The fatigue test results of less than 10^6 cycles were significantly influenced by the surface conditions of the as-manufactured specimen. Liu *et al.*[27] reported

that in the engineering applications, surface defects influence the low-cycle fatigue, whereas internal defects are dominant in the high-cycle fatigue. For engineering applications, Sun *et al.*[28] compared the fatigue behaviors of CPTi and Ti64 in a very high cycle range from 10^5 to 10^8. However, clinically important low-cycle fatigue data are lacking. This study provides practical fatigue data for clasps in terms of the comparison between CPTi and Ti64 from 10^4 to 10^6 cycles. However, the influence of the surface roughness and defects[27] should be studied further using post-treatment in future.

A significant study on the fatigue behavior of AM CPTi was conducted by Hasib *et al.*[29]. They discussed the correlation between the building orientation in LPBF and fatigue. It was proposed that the building orientation influenced the fatigue properties when the crack extension speed was low. To fabricate the specimens in this study, a limitation existed in determining the building orientation because of the cylindrical chucking part. Kobayashi *et al.*[30] presented the dependency of the shape error and internal defects on the building orientation for Co–Cr. Wang *et al.*[31] discussed the support structures of partial dentures. In the next step of the present study, the same building orientation as that of a clinical clasp[20] without the cylindrical chucking part would be used by developing a geometry compensation methodology[32] for the chucking part.

In addition to the experimental data, a numerical approach was presented to predict the fatigue life. The usefulness of FEA for prosthesis design is well established[33,34]. However, to the best of our knowledge, the prediction of the fatigue life of additively manufactured clasps has not yet been published. The fracture position in the fatigue test is in the region of stress concentration in the FEA, which supports the usefulness of FEA. Notably, a highly accurate 10-node quadratic-type element and fine mesh were employed, as shown in **Figure 4b**. Based on the SWT method, which is widely used for titanium and aluminum alloys[35], and the Baumel and Seeger rule, the parameters were calibrated for CPTi and Ti64. In future, they must be validated through experiments on clasps with different shapes. That is, using the calibrated parameters listed in **Table 3**, the FEA and fatigue life prediction of a clasp with different sizes must be performed and compared with the experimental results. In such a validation study leading to the generalization of the methodology, the variability in the fatigue life should be thoroughly analyzed by increasing the number of fatigue tests. Within this limitation, the present results allow us to evaluate the fatigue life in the design phase before manufacturing. This is important for ensuring the quality of the patient-specific clasp.

Repeatability is an important and critical factor in AM and LPBF[36] for the quality assurance of clasps for clinical use. In the experimental results, variability was observed for higher strokes; however, under smaller strokes, no variability was observed, although the number of specimens was limited. The sources of variability are the material properties, geometrical accuracy, and initial defects in the AM clasp. Concerning the material properties, the ultimate strength of Ti64 listed in **Table 1** is consistent with the average level reported by Dowling *et al.*[37]. FEA can predict the fatigue life before manufacturing, as shown in **Figure 8**. To analyze the variability, novel numerical studies have considered the initial defects in probabilistic FEA[18–20,38]. However, the variability in the fatigue life can be expressed by calibrating the fatigue parameters in the SWT method, in a similar manner as that performed for the averaged fatigue life in **Figure 8 and Table 3**.

5. Conclusions

CPTi and Ti64 clasps in a typical design of Akers were manufactured using LPBF. Specimens uniquely designed for chucking in a stroke-controlled fatigue testing machine were used. Fourteen fatigue tests were conducted for each material. Within the limitations of this study, the experimental results based on the N25 test method revealed that the CPTi clasp exhibited a longer fatigue life than the Ti64 clasp under a stroke smaller than 0.33 mm.

In the numerical studies, the elastoplastic material model was determined using a static tensile test of dumbbell-type flat plate specimens manufactured via LPBF. The stress concentration region estimated using FEA was consistent with the fracture position in the experiment. The parameters in the SWT method were calibrated for CPTi and Ti64. Under the limitations of the above-mentioned clasp design and cyclic loading condition, the establishment of the numerical method enabled us to predict the fatigue life and analyze quality assurance in the design phase before manufacturing. The application of this method to other clasp designs will be validated in the next step.

Acknowledgments

This study was supported by the JSPS Grants in Aid for Scientific Research B (20H02034). The authors acknowledge the help of a former student at Keio University, Mr. Ryo Nagami, for performing the fatigue test of the titanium alloy.

Conflict of interest statement

There are no conflicts of interest to declare in regard to this study.

References

[1] Jiménez A, Bidare P, Hassanin H, Tarlochan F, Dimov S, Essa K. Powder-based laser hybrid additive manufacturing of metals: a review. Int J Adv Manuf Technol. 2021;114:63–96. https://doi.org/10.1007/s00170-021-06855-4

[2] Diegel O, Nordin A, Motte DA. Practical Guide to Design for Additive Manufacturing. Springer; 2020.

[3] Thompson MK, Moroni G, Vaneker T, Fadel G, Campbell RI, Gibson I, *et al.* Design for Additive Manufacturing: Trends, opportunities, considerations, and constraints. CIRP Ann. 2016;65:737–60. https://doi.org/10.1016/j.cirp.2016.05.004

[4] Al Jabbari YS. Physico-mechanical properties and prosthodontic applications of Co-Cr dental alloys: a review of the literature. J Adv Prosthodont. 2014;6:138–45. https://doi.org/10.4047/jap.2014.6.2.138, PMID:24843400

[5] Cheng H, Xu M, Zhang H, Wu W, Zheng M, Li X. Cyclic fatigue properties of cobalt-chromium alloy clasps for partial removable dental prostheses. J Prosthet Dent. 2010;104:389–96. https://doi.org/10.1016/S0022-3913(10)60173-4, PMID:21095402

[6] Marie A, Keeling A, Hyde TP, Nattress BR, Pavitt S, Murphy RJ, *et al.* Deformation and retentive force following in vitro cyclic fatigue of cobalt-chrome and aryl ketone polymer (AKP) clasps. Dent Mater. 2019;35:e113–21. https://doi.org/10.1016/j.dental.2019.02.028, PMID:30948229

[7] Yager S, Ma J, Ozcan H, Kilinc HI, Elwany AH, Karaman I. Mechanical properties and microstructure of removable partial denture clasps manufactured using selective laser melting. Addit Manuf. 2015;8:117–23. https://doi.org/10.1016/j.addma.2015.09.005

[8] Tasaka A, Kato Y, Odaka K, Matsunaga S, Goto T, Abe S, *et al.* Accuracy of clasps fabricated with three different CAD/CAM technologies: casting, milling, and selective laser sintering. Int J Prosthodont. 2019;32:526–9. https://doi.org/10.11607/ijp.6363, PMID:31664269

[9] Takaichi A, Fueki K, Murakami N, Ueno T, Inamochi Y, Wada J, *et al.* A systematic review of digital removable partial dentures. Part II: CAD/CAM framework, artificial teeth, and denture base. J Prosthodont Res. 2022;66:53–67. https://doi.org/10.2186/jpr.JPR_D_20_00117, PMID:33504722

[10] Suzuki Y, Shimizu S, Waki T, Shimpo H, Ohkubo C. Laboratory efficiency of additive manufacturing for removable denture frameworks: A literature-based review. Dent Mater J. 2021;40:265–71. https://doi.org/10.4012/dmj.2020-206, PMID:33361665

[11] Kato Y, Tasaka A, Kato M, Wadachi J, Takemoto S, Yamashita S. Effects of repetitive insertion/removal cycles and simulated occlusal loads on retention of denture retainers. Dent Mater J. 2021;40:1277–83. https://doi.org/10.4012/dmj.2020-462, PMID:33883331

[12] Zhang M, Gan N, Qian H, Jiao T. Retentive force and fitness accuracy of cobalt-chrome alloy clasps for removable partial denture fabricated with SLM technique. J Prosthodont Res. 2022;66:459–65. https://doi.org/10.4012/dmj.2020-462 , PMID:33883331

[13] Schweiger J, Güth JF, Erdelt KJ, Edelhoff D, Schubert O. Internal porosities, retentive force, and survival of cobalt–chromium alloy clasps fabricated by selective laser-sintering. J Prosthodont Res. 2020;64:210–6. https://doi.org/10.1016/j.jpor.2019.07.006, PMID:31680054

[14] Dong YP, Tang JC, Wang DW, Wang N, He ZD, Li J, *et al.* Additive manufacturing of pure Ti with superior mechanical performance, low cost, and biocompatibility for potential replacement of Ti-6Al-4V. Mater Des. 2020;196:109142. https://doi.org/10.1016/j.matdes.2020.109142

[15] Mahmoud A, Wakabayashi N, Takahashi H, Ohyama T. Deflection fatigue of Ti-6Al-7Nb, Co-Cr, and gold alloy cast clasps. J Prosthet Dent. 2005;93:183–8. https://doi.org/10.1016/j.prosdent.2004.11.011, PMID:15674231

[16] Takayama Y, Takishin N, Tsuchida F, Hosoi T. Survey on use of titanium dentures in Tsurumi University Dental Hospital for 11 years. J Prosthodont Res. 2009;53:53–9. https://doi.org/10.1016/j.jpor.2008.08.011, PMID:19318073

[17] Takahashi K, Torii M, Nakata T, Kawamura N, Shimpo H, Ohkubo C. Fitness accuracy and retentive forces of additive manufactured titanium clasp. J Prosthodont Res. 2020;64:468–77. https://doi.org/10.1016/j.jpor.2020.01.001, PMID:32063534

[18] Takano N, Takizawa H, Wen P, Odaka K, Matsunaga S, Abe S. Stochastic prediction of apparent compressive stiffness of selective laser sintered lattice structure with geometrical imperfection and uncertainty in material property. Int J Mech Sci. 2017;134:347–56. https://doi.org/10.1016/j.ijmecsci.2017.08.060

[19] Maruno M, Takano N. Probabilistic prediction of mechanical behavior of additively manufactured product considering geometrical imperfections associated with building direction. Mechanical Engineering Journal. 2021;8:21-00288. https://doi.org/10.1299/mej.21-00288

[20] Odaka K, Takano N, Takizawa H, Matsunaga S. Probabilistic finite element analysis of fatigue life of additively manufactured clasp. Dent Mater J. 2022;41:286–94. https://doi.org/10.4012/dmj.2021-174, PMID:35249900

[21] Wu C, Zheng K, Fang J, Steven GP, Li Q. Time-dependent topology optimization of bone plates considering bone remodeling. Comput Methods Appl Mech Eng. 2020;359:112702. https://doi.org/10.1016/j.cma.2019.112702

[22] Smith KN, Watson P, Topper TH. A stress-strain function for the fatigue of metals. J Mater. 1970;5:767–78.

[23] Baumel A, Seeger T. Material Data for Cyclic Loading, Supplement 1, Elsevier Science Publishers, 1990.

[24] Tan FB, Song JL, Wang C, Fan YB, Dai HW. Titanium clasp fabricated by selective laser melting, CNC milling, and conventional casting: a comparative in vitro study. J Prosthodont Res. 2019;63:58–65. https://doi.org/10.1016/j.jpor.2018.08.002, PMID:30309743

[25] Fueki K, Inamochi Y, Wada J, Arai Y, Takaichi A, Murakami N, *et al.* A systematic review of digital removable partial dentures. Part I: clinical evidence, digital impression, and maxillomandibular relationship record. J Prosthodont Res. 2022;66:40–52. https://doi.org/10.2186/jpr.JPR_D_20_00116, PMID:33504721

[26] De Wild M, Ghayor C, Zimmermann S, Ruegg J, Nicholls F, Schuler F, Chen TH, Weber FE. Osteoconductive lattice microarchitecture for optimized bone regeneration. 3D Printing and Additive Manufacturing. 2019;6:40-9. https://doi.org/10.1089/3dp.2017.0129

[27] Liu S, Shin YC. Additive manufacturing of Ti6Al4V alloy: A review. Mater Des. 2019;164:107552. https://doi.org/10.1016/j.matdes.2018.107552

[28] Sun C, Chi W, Wang W, Duan Y. Characteristic and mechanism of crack initiation and early growth of an additively manufactured Ti-6Al-4V in very high cycle fatigue regime. Int J Mech Sci. 2021;205:106591. https://doi.org/10.1016/j.ijmecsci.2021.106591

[29] Hasib MT, Ostergaard HE, Liu Q, Li X, Kruzic JJ. Tensile and fatigue crack growth behavior of commercially pure titanium produced by laser powder bed fusion additive manufacturing. Addit Manuf. 2021;45:102027. https://doi.org/10.1016/j.addma.2021.102027

[30] Kobayashi H, Tasaka A, Higuchi S, Yamashita S. Influence of molding angle on the trueness and defects of removable partial denture frameworks fabricated by selective laser melting. J Prosthodont Res. 2021;66:589-99. https://doi.org/10.2186/jpr.JPR_D_21_00175 ,

[31] Wang Z, Zhang Y, Tan S, Ding L, Bernard A. Support point determination for support structure design in additive manufacturing. Addit Manuf. 2021;47:102341. https://doi.org/10.1016/j.addma.2021.102341

[32] Hong R, Zhang L, Lifton J, Daynes S, Wei J, Feih S, *et al.* Artificial neural network-based geometry compensation to improve the printing accuracy of selective laser melting fabricated sub-millimetre overhang trusses. Addit Manuf. 2021;37:101594. https://doi.org/10.1016/j.addma.2020.101594

[33] Sandu L, Faur N, Bortun C. Finite element stress analysis and fatigue behavior of cast circumferential clasps. J Prosthet Dent. 2007;97:39–44. https://doi.org/10.1016/j.prosdent.2006.11.003, PMID:17280890

[34] Yamaguchi S, Yamanishi Y, Machado LS, Matsumoto S, Tovar N, Coelho PG, *et al.* In vitro fatigue tests and in silico finite element analysis of dental implants with different fixture/abutment joint types using computer-aided design models. J Prosthodont Res. 2018;62:24–30. https://doi.org/10.1016/j.jpor.2017.03.006, PMID:28427837

[35] Schneller W, Leitner M, Pomberger S, Grün F, Leuders S, Pfeifer T, *et al.* Fatigue strength assessment of additively manufactured metallic structures considering bulk and surface layer characteristics. Addit Manuf. 2021;40:101930. https://doi.org/10.1016/j.addma.2021.101930

[36] Huang DJ, Li H. A machine learning guided investigation of quality repeatability in metal laser powder bed fusion additive manufacturing. Mater Des. 2021;203:109606. https://doi.org/10.1016/j.matdes.2021.109606

[37] Dowling L, Kennedy J, O'Shaughnessy S, Trimble D. A review of critical repeatability and reproducibility issues in powder bed fusion. Mater Des. 2020;186:108346. https://doi.org/10.1016/j.matdes.2019.108346

[38] Bercelli L, Moyne S, Dhondt M, Doudard C, Calloch S, Beaudet J. A probabilistic approach for high cycle fatigue of Wire and Arc Additive Manufactured parts taking into account process-induced pores. Addit Manuf. 2021;42:101989. https://doi.org/10.1016/j.addma.2021.101989